Internal Medicine
The Japanese Society of Internal Medicine
doi: 10.2169/internalmedicine.3577-19
Intern Med 59: 365-372, 2020
http://internmed.jp

【 CASE REPORT 】

Poorly Differentiated Hepatocellular Carcinoma in a Low-risk Patient with an Otherwise Normal Liver

Nobuhiko Ogasawara[1], Satoshi Saitoh[1], Hideyuki Denpou[2], Keiichi Kinowaki[3], Norio Akuta[1], Fumitaka Suzuki[1], Masashi Hashimoto[4], Shunichiro Fujiyama[1], Yusuke Kawamura[1], Hitomi Sezaki[1], Tetsuya Hosaka[1], Masahiro Kobayashi[1], Yoshiyuki Suzuki[1], Yasuji Arase[1], Kenji Ikeda[1], Takeshi Fujii[3] and Hiromitsu Kumada[1]

Abstract:
We herein report a 48-year-old healthy woman who visited our hospital to investigate a 25-mm space-occupying lesion in the liver. The tumor was irregularly shaped and exhibited heterogeneous enhancement on dynamic computed tomography (CT). Whole-body positron emission tomography-CT showed an abnormal fluorodeoxyglucose uptake in the liver tumor, with a maximum standardized uptake value of 12.82. During the ensuing three months, the tumor grew rapidly and the serum alpha-fetoprotein levels also rose; partial hepatectomy was therefore performed. Microscopic findings revealed a moderately-to-poorly differentiated hepatocellular carcinoma in the normal liver.

Key words: poorly differentiated hepatocellular carcinoma, normal liver, risk factors, alpha-fetoprotein

(Intern Med 59: 365-372, 2020)
(DOI: 10.2169/internalmedicine.3577-19)

Introduction

The most common etiology of hepatocellular carcinoma (HCC) in Japan and most other countries is chronic infection with hepatitis B virus (HBV) or hepatitis C virus (HCV) (1). Diabetes mellitus, alcoholism, metabolic syndrome, and obesity have also been implicated in HCC development (2-5). In addition, advanced age and male sex are important risk factors for HCC (6).

We herein report a case of poorly differentiated HCC discovered in the normal liver of a healthy, relatively young woman.

Case Report

A 48-year-old woman visited our hospital to investigate a 25-mm space-occupying lesion in the liver that had been detected by abdominal ultrasonography during a medical checkup 3 months earlier. She had undergone medical checkups annually, and no abnormalities had been observed before her most recent visit. She had no remarkable medical history and did not smoke or drink alcohol. Furthermore, she was not taking any medications and had also never taken oral contraceptives. During the three-month follow-up period, the tumor grew in size, whereupon she was admitted to the Department of Hepatology.

Her body mass index was 18.7 kg/m^2, and there were no abnormal physical findings. Blood tests on admission showed no viral infection, such as HBV or HCV infection; however, she had a high serum level of alpha-fetoprotein (AFP; 224 ng/mL) and AFP-L3 isoform ratio (51.1%). All laboratory data are summarized in Table 1.

Dynamic computed tomography (CT) performed three months before admission showed an 11×25-mm, irregularly shaped lesion with heterogeneous enhancement in S6 of the liver (Fig. 1). On ethoxybenzyl (EOB)-magnetic resonance imaging (MRI) performed two months before admission, the tumor had been the same size and shown heterogeneously elevated T2-weighted and diffusion-weighted signal intensi-

[1]Department of Hepatology, Toranomon Hospital, Japan, [2]Department of Clinical Laboratory, Toranomon Hospital, Japan, [3]Department of Pathology, Toranomon Hospital, Japan and [4]Department of Gastrointestinal Surgery, Toranomon Hospital, Japan
Received: June 27, 2019; Accepted: September 1, 2019; Advance Publication by J-STAGE: October 17, 2019
Correspondence to Dr. Satoshi Saitoh, sa3110@f2.dion.ne.jp

Table 1. Laboratory Data of the Patient.

Peripheral blood		
White blood cells	3,800	/μL
Hemoglobin	9.2	g/dL
Platelets	32×10^4	/μL
Blood analysis		
Total protein	7.3	g/dL
Albumin	4.3	g/dL
Creatinine kinase	55	IU/L
Blood urea nitrogen	9	mg/dL
Creatinine	0.58	mg/dL
Total bilirubin	0.5	mg/dL
Aspartate aminotransferase	15	IU/L
Alanine aminotransferase	7	IU/L
Amylase	85	IU/L
Lactate dehydrogenase	128	IU/L
Alkaline phosphatase	164	IU/L
γ-glutamyl transpeptidase	12	IU/L
Triglyceride	57	mg/dL
Total cholesterol	206	mg/dL
High density lipoprotein	77	mg/dL
Low density lipoprotein	104	mg/dL
aPTT	24.4	s
PT	100.4	%
PT-INR	1	
Immunology		
Alpha-fetoprotein	224	ng/mL
Alpha-fetoprotein-L3	51.1	%
PIVKA-II protein	21	mAU/mL
Infection		
HBsAg	Negative	
HBsAb	Negative	
HBcAb	Negative	
HCV RNA	Negative	
HCV antibody	Negative	

aPTT: activated partial thromboplastin time, HBcAb: hepatitis B core antibody, HBsAb: hepatitis B surface antibody, HBsAg: hepatitis B surface antigen, HCV: hepatitis C virus, INR: international normalized ratio, PT: prothrombin time

ties with no uptake in the hepatobiliary phase (Fig. 2). Ultrasonography (US) performed one month before admission revealed a 25-mm mass lesion with almost uniformly low echogenicity projecting from the lower end of S6 in the liver (Fig. 3); the border was not clear, and the surface was irregular. Contrast-enhanced US (Sonazoid®) (CE-US) had shown hyper-enhancement that did not resemble a basket pattern in the arterial phase, with some areas of washout present in the portal vein phase. CE-US also showed uniform hypo-enhancement at the post-vascular phase (Fig. 4). Considering that the background liver tissue appeared to be normal, the differential diagnosis was a benign tumor, such as an angiomyolipoma or focal nodular hyperplasia.

However, dynamic CT on admission revealed that the tumor had grown to 17×34 mm (Fig. 5). The tumor size and AFP level doubling times were 48 and 52 days, respectively, which suggested that the tumor had been growing rapidly. We performed whole-body positron emission tomography CT (PET-CT) for a closer examination, which revealed an abnormal fluorodeoxyglucose uptake in the liver tumor with a maximum standardized uptake value (SUV_{max}) of 12.82 (Fig. 6). No metastatic lesions were detected elsewhere in the body. Considering the rapid tumor growth and elevated AFP level, the tumor was suspected of being HCC, and laparoscopic partial hepatectomy of S6 was performed.

Grossly, a multinodular mass was observed protruding from the liver surface (Fig. 7A). Various histologic patterns were observed, including a steatotic area with inflammatory infiltrate as well as a trabecular pattern with a pseudoglandular structure, suggesting a moderately differentiated HCC. Another area comprised large tumor cells with hyperchromatic nuclei arranged in a compact pattern, suggesting a poorly differentiated HCC (Fig. 7B-D). However, in the background (normal) liver tissue, no hepatocellular dysplasia, necroinflammatory lesions, portal fibrosis, steatosis, or iron deposition was observed (Fig. 7E, F). On immunohistochemistry, tumor cells in the poorly differentiated area were highly positive for glypican 3 and heat shock protein 70. Furthermore, the tumor cells were focally immunoreactive for hepatocyte paraffin 1, AFP, glutamine synthetase, and cytokeratin 19 but were negative for organic anion transporter 1B3 (OATP1B3) and exhibited no β-catenin nuclear translocation (Fig. 8). Taken together, these findings indicated a final diagnosis of poorly differentiated HCC of the normal liver: im(−), eg, Fc(+), Fc-inf(+), sf(+), s0, n0, vp0, vv0, va0, b0, p0, sm(−), 0 mm, nl, multinodular, 24×17×12 mm, pT1N0M0 stage I. The patient has remained well with no recurrence in the nine months since her surgery.

Discussion

Diagnosing this patient was very challenging, largely because HCC arising in a normal liver is extremely rare. HCC often arises as a complication of long-standing symptomatic cirrhosis mainly induced by HBV or HCV infection or else by excessive alcohol intake (7).

Cirrhosis is a major etiologic factor for the pathogenesis of HCC (7). Even in HCCs that arise in non-fibrotic livers, histopathologic analyses have frequently revealed minimal and nonspecific changes, including mild portal infiltration by mononuclear cells, mild iron overload, and mild microvascular steatosis (8). However, the examination of our patient revealed no such features. Only one case report referring to HCC arising in a normal liver exists in the PubMed database as of November 2018 when performing a search with the key words “hepatocellular carcinoma” and “normal liver” (9).

A second major reason for the difficulty in diagnosing our patient was that the HCC imaging characteristics were clearly different from typical imaging patterns normally observed in single nodular-type HCC, as described in Table 2. The typical imaging patterns on US are a lateral shadow, posterior echo enhancement, mosaic nodule-in-nodule pat-

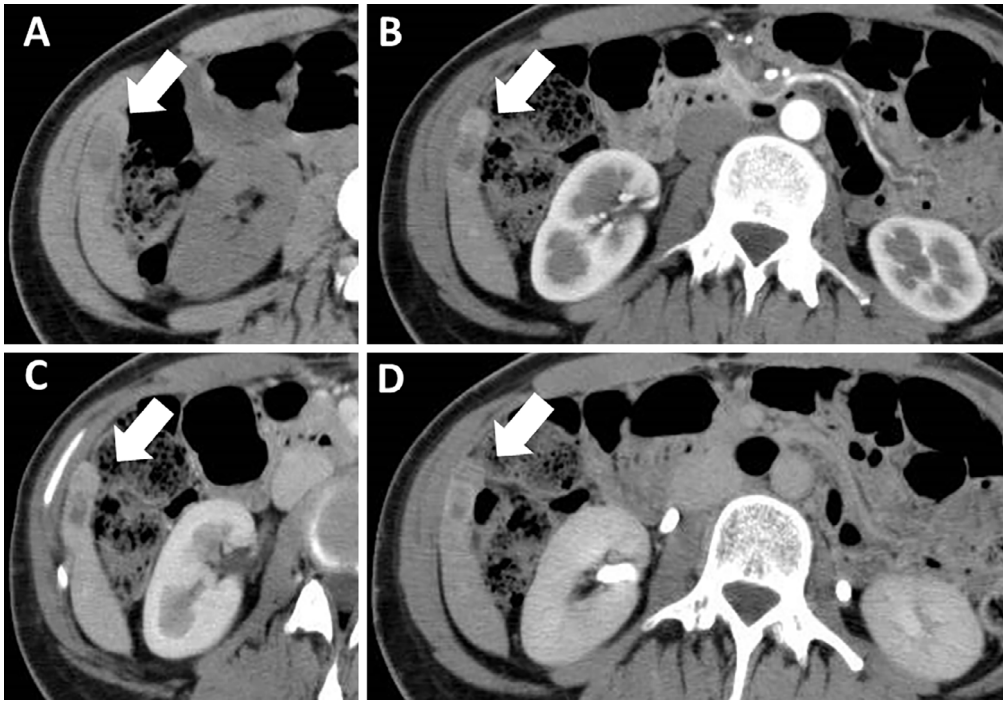

Figure 1. **Dynamic computed tomography performed 3 months before the patient's admission showed a 11×25-mm, irregularly shaped mass (arrows) (A). The lesion was heterogeneously enhanced during the arterial phase (B) and washed out during the portal vein phase (C). It also showed hypointensity at the equilibrium phase (D).**

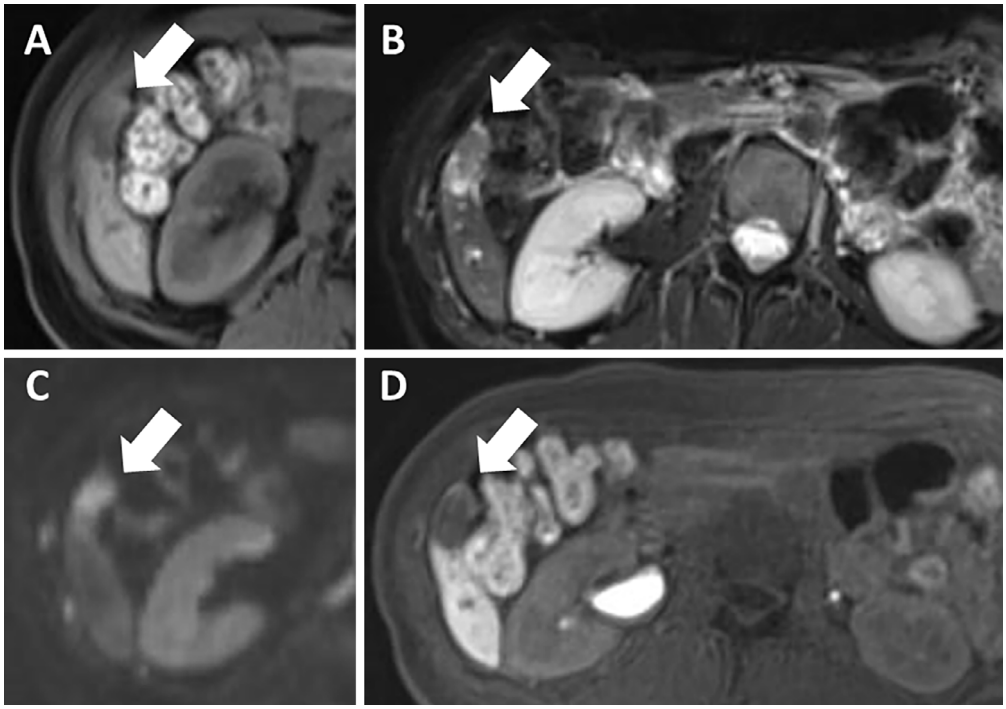

Figure 2. **On ethoxybenzyl-magnetic resonance imaging performed two months before the patient's admission, the tumor (arrows) had not changed in size and was isointense compared with the normal liver on T1-weighted imaging (T1WI) (A). It was also highly heterogeneous on T2-weighted imaging (T2WI) (B) and diffusion-weighted imaging (DWI) (C); there was no uptake in the hepatobiliary phase (D).**

tern, hyperechoic septum, and halo (10). Single nodular-type HCC has been described as showing 'basket pattern enhancement' on CE-US (11). Furthermore, the heterogeneously enhanced pattern of the tumor on CE-US and dynamic CT may represent a multinodular-type HCC with both moderate and poor differentiation. The atypical imaging charac-

teristics we observed in our patient may have been a consequence of the various histologic patterns of her tumor.

PET-CT has limited use as a diagnostic tool for HCC. A recent study showed that, because well- or moderately differentiated HCC may not have higher metabolic activity than the surrounding tissue, PET-CT does not necessarily reveal abnormalities in the hepatic lesions identified via CT (12).

It would be interesting to determine whether or not hepatocarcinogenesis in this case was *de novo* or involved multistep progression from dysplastic nodule to early HCC to classical HCC, as previously reported (13-15). It is difficult to determine this because we do not have the imaging results of her past medical checkups. However, considering that the tumor included both moderately and poorly differentiated HCC and that fat lesions are less frequent in *de novo* HCC than in multistep HCC (16), hepatocarcinogenesis in this case may have involved multistep progression.

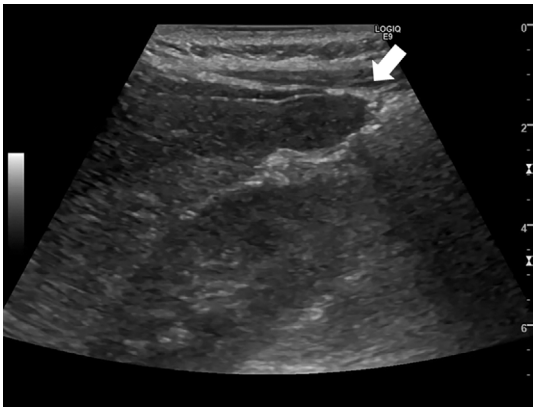

Figure 3. Abdominal ultrasonography performed 1 month before the patient's admission showed a 25-mm uniformly low-echoic mass projecting from the lower end of S6 in the liver (arrow). The border was not clear, and the surface was irregular.

A major concern is our patient's prognosis, given that her HCC was poorly differentiated. Chen et al. showed that the SUV_{max} is higher in patients with poorly differentiated HCC than in those with well- or moderately differentiated counterparts; the median SUV_{max} of poorly differentiated HCCs in their study was 6.7 (17), while that of our patient was much higher at 12.82. Indeed, the area in the liver tumor showing an abnormal fluorodeoxyglucose uptake corresponded with the hypovascular area detected on dynamic CT, which suggested that this area could have high malignancy. Furthermore, the uptake of fluorodeoxyglucose on PET-CT is reported to be an independent predictor of early recurrence after surgery for HCC (18). In general, the EOB-MRI uptake in the hepatobiliary phase is correlated with low serum AFP levels, maintenance of the hepatocyte function with the upregulation of OATP1B3 expression, and a good prognosis. In contrast, HCC showing a reduced uptake in the hepatobiliary phase with high serum AFP levels was shown to be associated with a poor prognosis (19). In our patient, the tumor had a reduced uptake in the hepatobiliary phase with high serum AFP levels, and the OATP1B3 expression was lacking. Based on these data, our patient's prognosis is expected to be poor, with the early recurrence of HCC. Although the patient has remained well with no recurrence during the nine months since her surgery, she will require close observation from now on.

Our episode exemplifies how HCC can emerge even in the normal liver of a relatively young and healthy person who has minimal risk of this disease. The possibility of a poorly differentiated HCC should therefore be taken into consideration when encountering a hepatic lesion with atypical imaging characteristics.

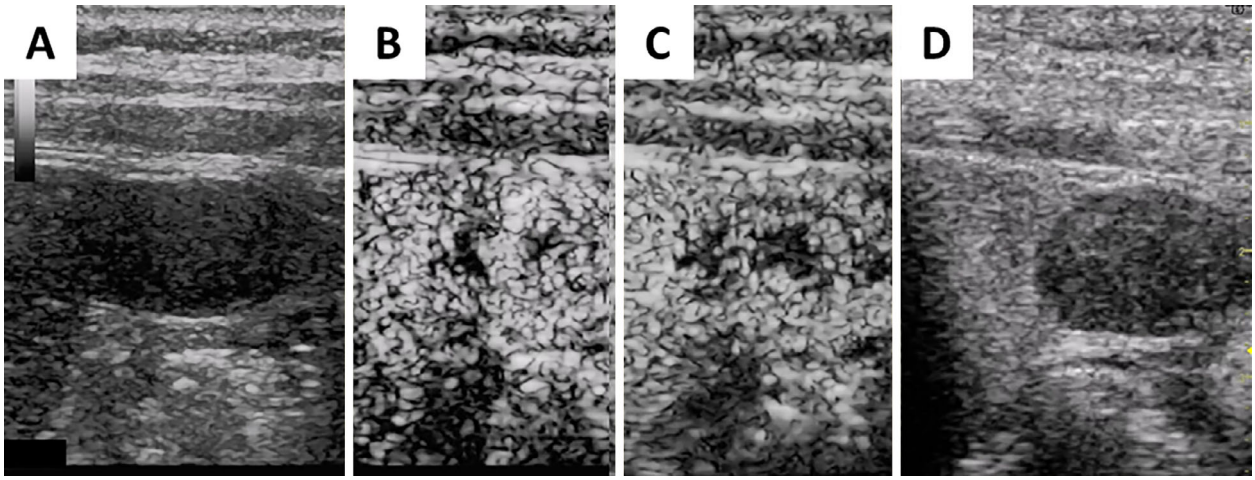

Figure 4. Before intravenous bolus, the tumor was revealed to be a uniformly low-echoic and irregularly shaped projecting mass (A). Contrast-enhanced ultrasonography (Sonazoid®) showed that the tumor with hyper enhancement did not have a basket pattern at the arterial phase (B), with some areas of the tumor being washed out in the portal vein phase (C). Sonazoid-enhanced ultrasonography also showed uniform hypoenhancement in the tumor at the post-vascular phase (D).

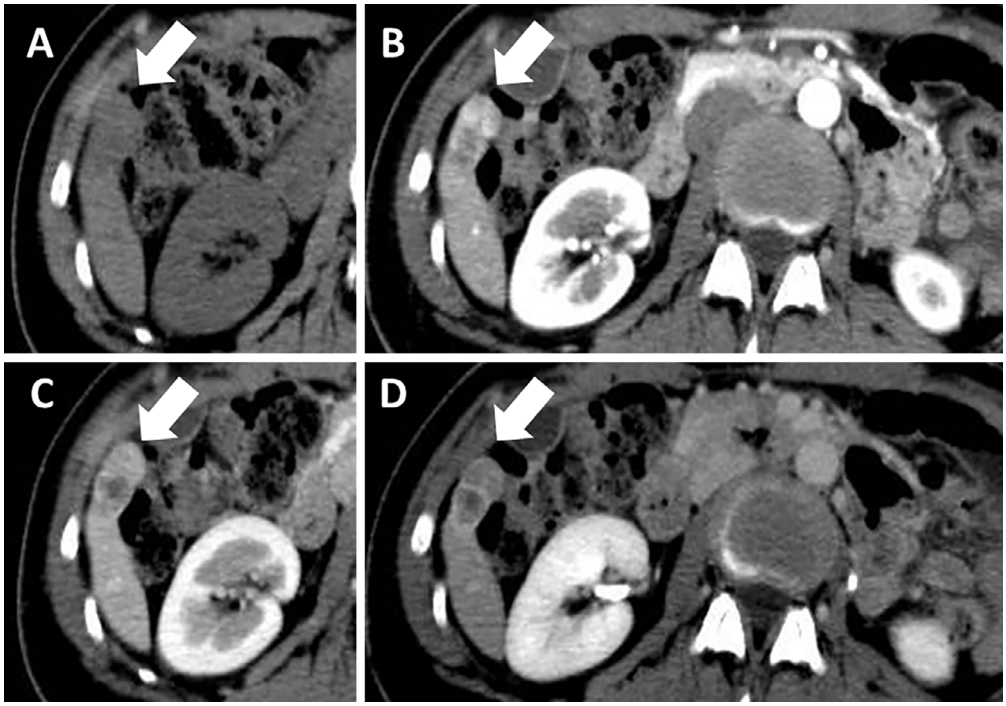

Figure 5. **Dynamic computed tomography at the time of admission showed an enlarged tumor (17×34 mm; arrows) (A). The lesion was heterogeneously enhanced during the arterial phase (B) and washed out during the portal vein phase (C). It also presented as a hypointense lesion at the equilibrium phase (D).**

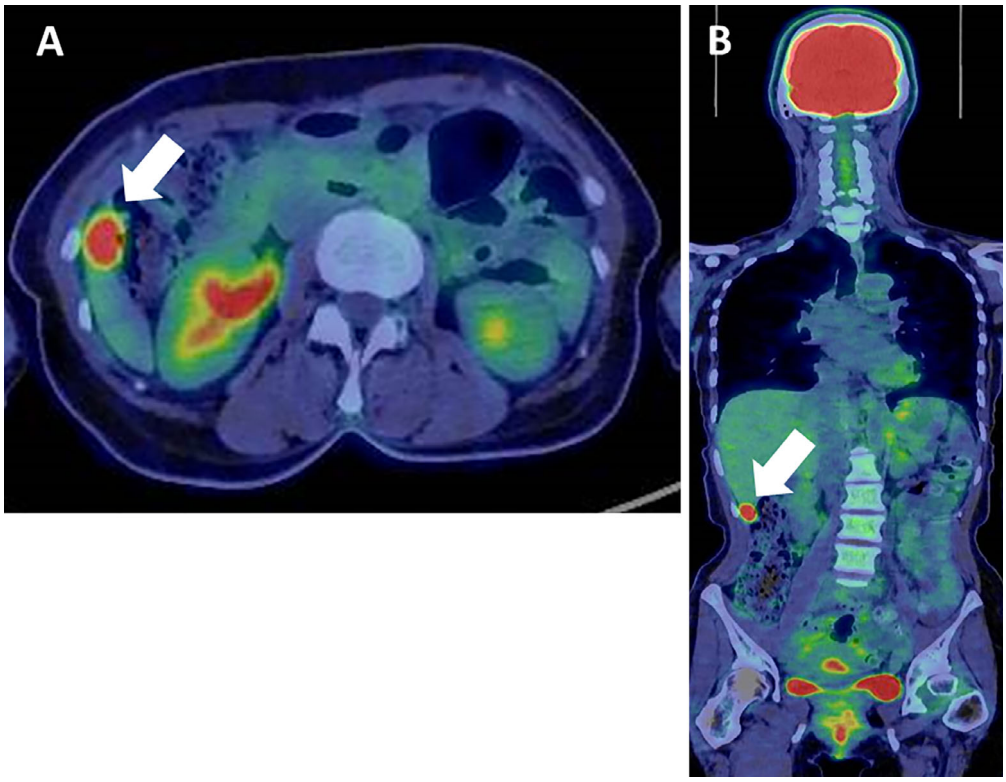

Figure 6. **Whole-body positron emission tomography-computed tomography showed an abnormal fluorodeoxyglucose uptake in the liver tumor, with a maximum standardized uptake value of 12.82 (A). No metastases were detected elsewhere (B).**

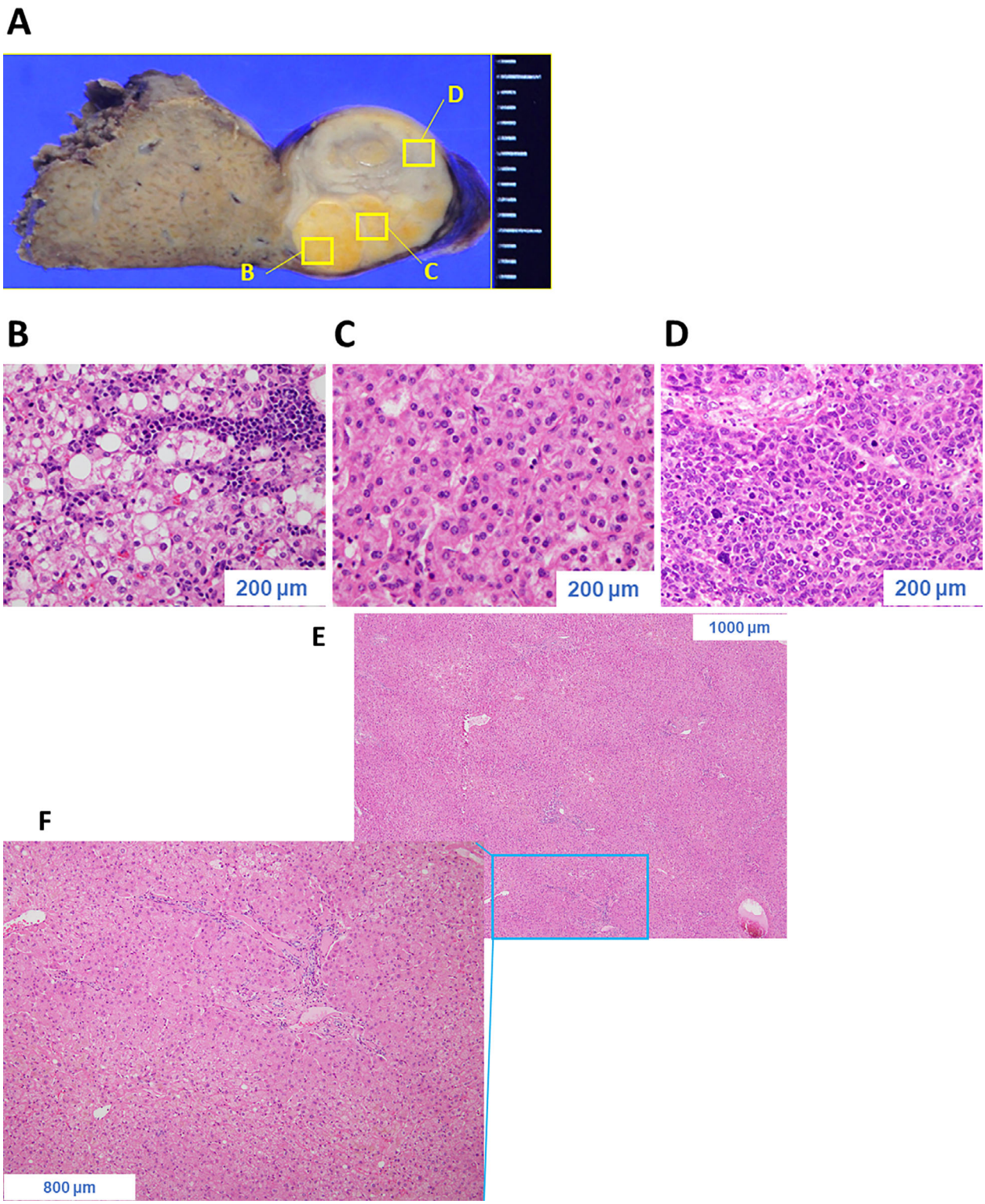

Figure 7. **Grossly, the tumor presented as a multinodular mass protruding from the liver surface (A). Histologically, various patterns were observed, including steatotic areas with inflammatory infiltrate (B), a trabecular pattern with pseudoglandular structure (C), and an area comprising large tumor cells with hyperchromatic nuclei arranged in a compact pattern (D). In the background liver tissue, no hepatocellular dysplasia, necroinflammatory lesions, portal fibrosis, steatosis, or iron deposition was observed (E, F).**

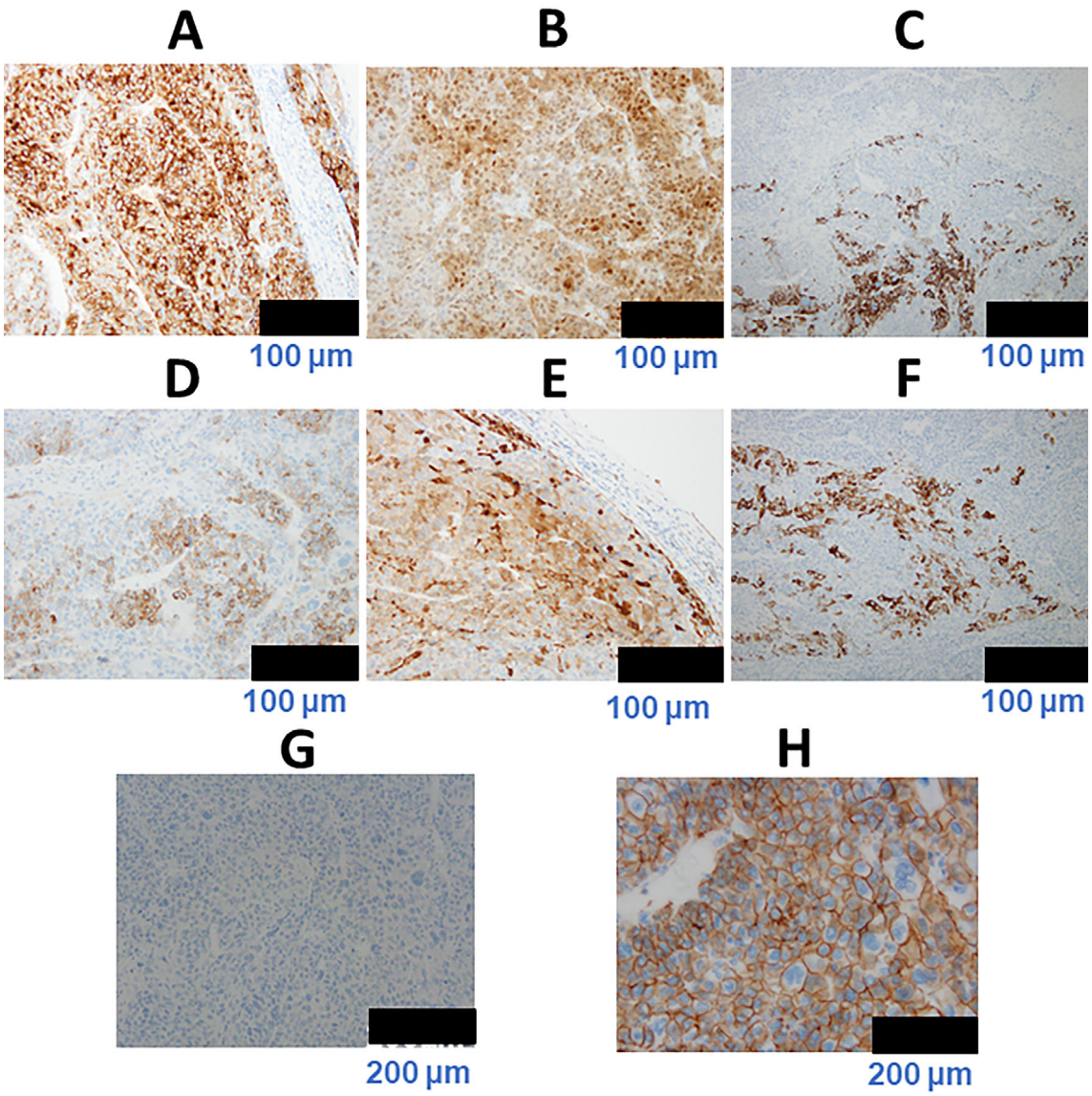

Figure 8. **On immunohistochemistry, the tumor cells in the poorly differentiated area were highly immunoreactive for glypican 3 (GPC3) (A) and heat shock protein 70 (HSP70) (B). Furthermore, the tumor cells were focally immunoreactive for hepatocyte paraffin 1 (HepPar1) (C), alpha-fetoprotein (AFP) (D), glutamine synthetase (GS) (E), and cytokeratin 19 (CK19) (F) but were negative for organic anion transporter 1B3 (OATP1B3) (G). No β-catenin nuclear translocation was observed (H).**

Table 2. **Comparison between Typical HCC Characteristics and Our Patient's Tumor Characteristics.**

Imaging	Current patient	Single nodular-type HCC (Naive)	Reference
US	Elliptical shape	Round shape	(10)
	Unclear border	Well-defined border	
	Irregular outline	Regular outline	
	Homogenous echogenicity	Heterogeneous echogenicity	
	Without low echoic septum	Low echoic septum	
	Without nodule-in-nodule	Nodule-in-nodule	
	Without lateral shadow	Lateral shadow	
CE-US	Non-basket pattern enhancement	Basket pattern enhancement	(11)
PET-CT	Positive (high SUV_{max})	Negative (low SUV_{max})	(12)

HCC: hepatocellular carcinoma, PET-CT: positron emission tomography-computed tomography, CE-US: Contrast-enhanced ultrasonography (Sonazoid®), SUV_{max}: maximum standardized uptake value, US: ultrasonography

Author's disclosure of potential Conflicts of Interest (COI).
Norio Akuta: Honoraria, Bristol-Myers Squibb and AbbVie. Yoshiyuki Suzuki: Honoraria, Bristol-Myers Squibb and AbbVie. Hiromitsu Kumada : Honoraria, MSD, Bristol-Myers Squibb, Gilead Sciences, AbbVie and Dainippon Sumitomo Pharma.

References

1. Yuen MF, Hou JL, Chutaputti A; Asia Pacific Working Party on Prevention of Hepatocellular Carcinoma. Hepatocellular carcinoma in the Asia Pacific region. J Gastroenterol Hepatol **24**: 346-353, 2009.
2. El-Serag HB, Tran T, Everhart JE. Diabetes increases the risk of chronic liver disease and hepatocellular carcinoma. Gastroenterology **126**: 460-468, 2004.
3. Davila JA, Morgan RO, Shaib Y, McGlynn KA, El-Serag HB. Diabetes increases the risk of hepatocellular carcinoma in the United States: a population-based control study. Gut **54**: 533-539, 2005.
4. Polesel J, Zucchetto A, Monella M, et al. The impact of obesity and diabetes mellitus on the risk of hepatocellular carcinoma. Ann Oncol **20**: 353-357, 2009.
5. Tateishi R, Uchino K, Fujikawa N, et al. A nationwide survey on non-B, non-C hepatocellular carcinoma in Japan: 2011-2015 update. J Gastroenterol **54**: 367-376, 2019.
6. Li TC, Li CI, Liu CS, et al. Risk score system for the prediction of hepatocellular carcinoma in patients with type 2 diabetes: Taiwan Diabetes Study. Semin Oncol **45**: 264-274, 2018.
7. Tang A, Hallouch O, Chemyak V, Kamaya A, Sirlin CB. Epidemiology of hepatocellular carcinoma: target population for surveillance and diagnosis. Abdom Radiol **43**: 13-25, 2018.
8. Bralet MP, Regimbeau JM, Pineau P, et al. Hepatocellular carcinoma occurring in nonfibrotic liver: epidemiologic and histopathologic analysis of 80 French cases. Hepatology **32**: 200-204, 2000.
9. Komiyama S, Okazaki H, Nakao S, et al. Diffuse fatty metamorphosis of a large, well-differentiated hepatocellular carcinoma originating in the normal liver: a case report and literature review. Clin J Gastroenterol **8**: 345-350, 2015.
10. Bialecki ES, Di Bisceglie AM. Diagnosis of hepatocellular carcinoma. HPB (Oxford) **7**: 26-34, 2005.
11. Catalano O, Nunziata A, Lobianco R, Siani A. Real-time harmonic contrast materialspecific US of focal liver lesions. Radiographics **25**: 333-349, 2005.
12. Liangpunsakul S, Agarwal D, Horlander JC, Kieff B, Chalasani N. Positron emission tomography for detecting occult hepatocellular carcinoma in hepatitis C cirrhotics awaiting for liver transplantation. Transplant Proc **35**: 2995-2997, 2003.
13. Matsui O. Imaging of multistep human hepatocarcinogenesis by CT during intra-arterial contrast injection. Intervirology **47**: 271-276, 2004.
14. Kudo M. Multistep human hepatocarcinogenesis: correlation of imaging with pathology. J Gastroenterol **44**: 112-118, 2009.
15. Kitao A, Zen Y, Matsui O, et al. Hepatocarcinogenesis: multistep changes of drainage vessels at CT during arterial portography and hepatic arteriography-radiologic-pathologic correlation. Radiology **252**: 605-614, 2009.
16. Tamada T, Korenaga M, Ito K, et al. Assessment of clinical and magnetic resonance imaging features of *de novo* hypervascular hepatocellular carcinoma using gadoxetic acid-enhanced magnetic resonance imaging. Hepatol Res **47**: 152-160, 2017.
17. Chen R, Li J, Zhou X, Liu J, Huang G. Fructose-1,6-bisphosphatase 1 reduces ^{18}F FDG uptake in hepatocellular carcinoma. Radiology **284**: 844-853, 2017.
18. Lim C, Salloum C, Chalaye J, et al. 18F-FDG PET/CT predicts microvascular invasion and early recurrence after liver resection for hepatocellular carcinoma: a prospective observational study. HPB (Oxford) **21**: 739-747, 2019.
19. Yamashita T, Kitao A, Matsui O, et al. Gd-EOB-DTPA-enhanced magnetic resonance imaging and alpha-fetoprotein predict prognosis of early-stage hepatocellular carcinoma. Hepatology **60**: 1674-1685, 2014.